Computer simulation of the packing of fine particles

R. Y. Yang, R. P. Zou, and A. B. Yu*
School of Materials Science and Engineering, The University of New South Wales, Sydney, New South Wales 2052, Australia
(Received 5 April 2000)

This paper presents a simulation study of the packing of uniform fine-spherical particles where the van der Waals force is dominant. It is shown that porosity increases with the decreases of particle size from about 100 to 1 μm and the simulated relationship can match the literature data well. The packing structure of fine particles is qualitatively depicted by illustrative pictures and quantified in terms of radial distribution function, angular distribution, and coordination number. The results indicate that in line with the increase in porosity, the first component of the split second peak and then the other peaks beyond the second one in the radial distribution function gradually vanish; the first peak becomes narrower, with a sharp decrease to the first minimum. As particle size decreases, the peaks at 120° and then 60° in the angular distribution will gradually vanish; the coordination number distribution shifts to the left and becomes narrower. The mean coordination number can decrease to a value as low as two for 1 μm particles, giving a very loose and chainlike structure. The interparticle forces acting on individual particles in a stable packing are analyzed and shown to be related to the packing properties.

PACS number(s): 61.43.Bn, 81.05.Rm, 61.43.Gt, 81.20.Ev

I. INTRODUCTION

Particle packing is of fundamental importance to many industries and has been subjected to research for many years [1,2]. It has also been found to be useful in modeling physical systems such as liquids [3] and amorphous materials [4]. Generally speaking, the studies in this area can be categorized into either (i) an assessment of the variables which govern the packing of particles at a macroscopic level, and subsequently, the development of methods for property and/or process control, or (ii) an examination of the structure of a packing of particles with particular reference to the pore and/or particle connectivity.

Macroscopic study is often focused on porosity and related parameters such as packing density and bulk density. Previous studies indicate that there are many factors affecting porosity [1,2]. Of particular practical interest are particle characteristics such as (dimensionless) particle size distribution, particle shape, and absolute particle size. These three factors can lead to various complex packing systems from mono- to multisized, spherical to nonspherical, and/or from coarse to fine particle packing. The understanding and modelling of the relationship between porosity and particle characteristics has been a subject of research since the turn of this century, namely, the classic work of Fuller and Thompson [5], progressing from the simple spherical particle packing to the complicated fine and nonspherical particle packing as recently reviewed by Yu and Zou [6]. In the 1980's significant progress has been made in this direction for coarse spherical particles [7–11]. Recently, this approach has been extended to the packing of coarse nonspherical particles [12–14].

When particle size is smaller than a certain value, the gravity is not the dominant force, and the interparticle force, which is the collective outcome of weak forces such as van der Waals and electrostatic forces, becomes more important [15]. Fine particles usually do not behave as individuals because of the formation of agglomerates due to the strong cohesive forces. Consequently, their packing behavior differs from that of coarse particles. This difference can be highlighted by the variation of porosity with particle size for monosized particles [2,16] and the open-tree packing structure observed under two-dimensional conditions or on the external surface of a packing [17,18]. Recently an attempt has been made to model this packing system with reference to alumina powder [19] but as a result of its empirical nature, the proposed model cannot be used generally [20]. Such limitation can be overcome only if a predictive method is developed based on a fundamental understanding of the packing of fine particles. Micromechanic analysis of particle packing is key to the development of such an understanding. Unfortunately, by now few publications deal with the packing structure of fine particles [21], although many efforts have been made on the packing of coarse particles [22,23].

Computer simulation has been widely used in the microscopic study of the packing of particles. Two techniques are widely used in the past: sequential (one-by-one) addition [24–34] and nonsequential (collective) rearrangement [35–43], involving different assumptions for packing growth and/or different criteria for stability. These assumptions or criteria are largely derived from geometrical consideration and applicable to the packing of coarse particles. They cannot be used in the simulation of the packing of fine particles, which depends on not only the gravity but also other interparticle forces such as the van der Waals and electrostatic forces. Proper incorporation of these forces in a computer simulation is key to generating realistic packing.

Dynamic simulation based on the so-called distinct element method (DEM) [44] is most effective in this regard, as it treats particle packing as a dynamic process where interparticle forces are explicitly considered. The usefulness of this simulation has been confirmed in our recent study of the

*Corresponding author. FAX: +61 2 9385 5956. Email address: a.yu@unsw.edu.au

 ©2000 The American Physical Society

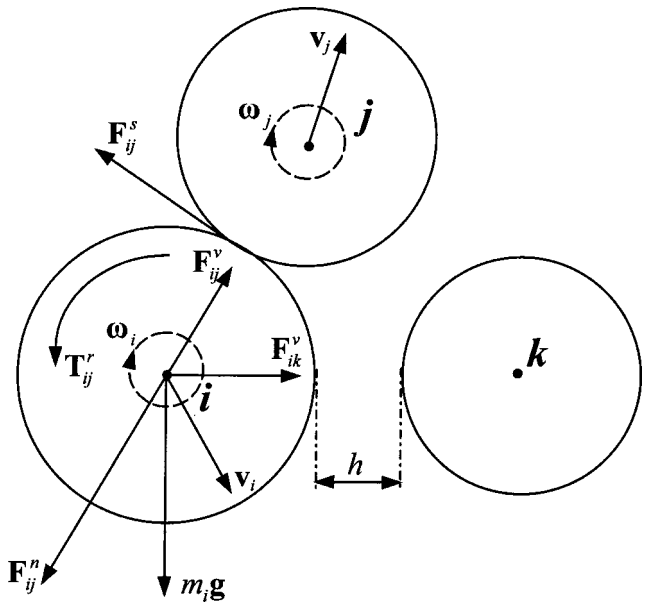

FIG. 1. Schematic illustration of the forces acting on particle i from contacting particle j and noncontacting particle k.

packing of coarse particles [45–47]. This paper extends that approach to the packing of fine particles where the van der Waals force is known to be dominant. It will be shown that the proposed simulation can generate results that are in good agreement with available experimental measurements and lead to the quantification of the structural properties of fine particles.

II. SIMULATION METHOD

A. Governing equations and calculation of interparticle forces

In general, a particle can possess two types of motion, namely, translational motion and rotational motion, which can be described by Newton's second law of motion, given by

$$m_i\frac{d\mathbf{v}_i}{dt}=\mathbf{F}_i, \tag{1}$$

$$I_i\frac{d\boldsymbol{\omega}_i}{dt}=\mathbf{T}_i, \tag{2}$$

where $\mathbf{v}_i$, ω_i, and I_i are, respectively, the translational and angular velocities, and moment of inertial of particle i; $\mathbf{F}_i$ and $\mathbf{T}_i$ represent the total force and total torque acting on the particle. For a particle of radius R_i and density ρ_i, its mass m_i and moment of inertial I_i are, respectively, given as $\frac{4}{3}\pi R_i^3\rho_i$ and $\frac{2}{5}m_iR_i^2$. Interparticle forces such as short-range contact forces as well as the long-range cohesive forces, including electrostatic force and the van der Waals force, are involved in a packing process. The present paper is concerned with particles larger than 1 μm, and for these particles the electrostatic force can be reasonably ignored [15,48]. Thus, as schematically illustrated in Fig. 1, the total force and torque on particle i are given by the following equations:

$$\mathbf{F}_i=\sum_j\ (\mathbf{F}_{ij}^n+\mathbf{F}_{ij}^s+\mathbf{F}_{ij}^v)+m_i\mathbf{g}, \tag{3}$$

$$\mathbf{T}_i=\sum_j\ (\mathbf{T}_{ij}^s+\mathbf{T}_{ij}^r), \tag{4}$$

where $\mathbf{F}_{ij}^n$, $\mathbf{F}_{ij}^s$, and $\mathbf{F}_{ij}^v$ represent, respectively, the normal contact force, tangential contact force, and the van der Waals force imposed on particle i by particle j; and $\mathbf{T}_{ij}^s$ and $\mathbf{T}_{ij}^r$ are the torques on particle i caused by tangential force $\mathbf{F}_{ij}^s$ and rolling friction. Once the forces involved are known, Eqs. (1) and (2) can be readily solved by the finite difference method, e.g., the so-called Verlet algorithm used in this paper [49].

The normal contact force consists of two components: an elastic, conservative component due to the deformation or overlap ξ_n and a viscous, dissipative component due to the dissipation of energy in the solid particle linked to normal impact velocity. Using the nonlinear Hertz model, the normal force acting on particle i, due to the collision with particle j, is given by [50,51]

$$\mathbf{F}_{ij}^n=[\tfrac{2}{3}E\sqrt{\overline{R}}\xi_n^{3/2}-\gamma_nE\sqrt{\overline{R}}\sqrt{\xi_n}(\mathbf{v}_{ij}\cdot\hat{\mathbf{n}}_{ij})]\hat{\mathbf{n}}_{ij}, \tag{5}$$

where parameter $E=Y/(1-\tilde{\sigma}^2)$, Y and $\tilde{\sigma}$ are the Young modulus and the Possion ratio, $\hat{\mathbf{n}}_{ij}$ is a unit vector runing from the center of particle j to the center of particle i, and $\overline{R}=R_iR_j/(R_i+R_j)$. The normal damping constant γ_n can be treated as a material property directly linked to the normal coefficient of restitution [47,52].

The relative motion between particles i and j in the contact surface (perpendicular to the normal direction) leads to a tangential force. This force opposes the motion of the interacting particles in the tangential direction and is given by [53,54]

$$\mathbf{F}_{ij}^s=-\mathrm{sgn}(\xi_s)\mu|\mathbf{F}_{ij}^n|\left[1-\left(1-\frac{\min(\xi_s,\xi_{s,\max})}{\xi_{s,\max}}\right)\right], \tag{6}$$

where μ is the friction coefficient, ξ_s is the total tangential displacement of particles during contact, and $\xi_{s,\max}=\mu[(2-\tilde{\sigma})/2(1-\tilde{\sigma})]\xi_n$ [54]. Equation (6) suggests when two particles start touching each other, a virtual spring is activiated in the tangential direction; and if $|\xi_s|>\xi_{s,\max}$, then gross sliding is deemed to have started, the virtual spring is detached, and the frictional force reduces to the Coulomb law of friction.

The torque on particle i due to the tangential force is $\mathbf{T}_{ij}^s=\mathbf{R}_i\times\mathbf{F}_{ij}^s$, where $\mathbf{R}_i$ is a vector runing from the center of the particle to the contact point with its magnitude equal to particle radius R_i. The contact between particles results in a rolling resistance due to elastic hysteresis losses or viscous dissipation [55,56], and this resistance plays a critical role in achieving physically or numerically stable results for unconfined packing, i.e., the formation of a sandpile [57]. In this work, the torque $\mathbf{T}_{ij}^r$ caused by this rolling friction is given by [56]

$$\mathbf{T}_{ij}^r=-\mu_rR_i|\mathbf{F}_{ij}^n|\hat{\boldsymbol{\omega}}_i, \tag{7}$$

where μ_r is the coefficient of rolling friction.

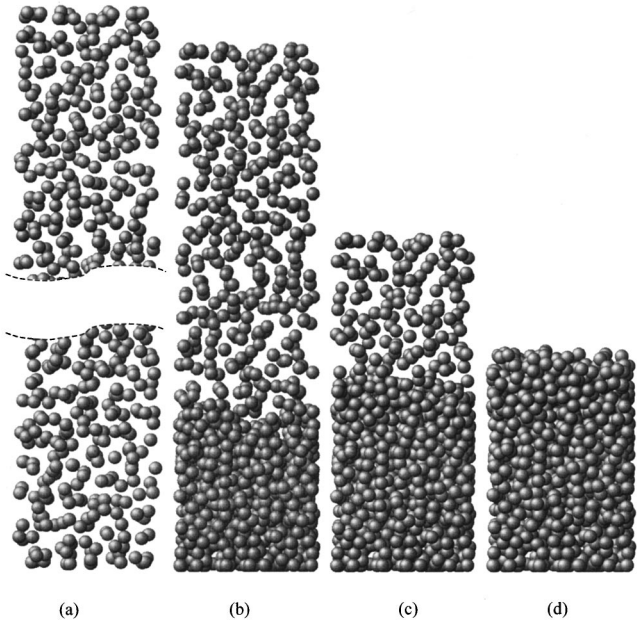

FIG. 2. Snapshots showing the formation of a packing of 5 μm particles at different times: (a) 0; (b) 0.06; (c) 0.08; and (d) 0.1 s.

As mentioned above, the only long-range, noncontact force considered in this paper is the van der Waals force. This force is given by [48,58]

$$\mathbf{F}_{ij}^{v} = -\frac{H_a}{6} \times \frac{64R_i^3R_j^3(h+R_i+R_j)}{(h^2+2R_ih+2R_jh)^2(h^2+2R_ih+2R_jh+4R_iR_j)^2}\hat{\mathbf{n}}_{ij}, \tag{8}$$

where H_a is the Hamaker constant, and h is the separation of surfaces along the line of the centers of particles i and j. While it is recognized that an overlap between two colliding particles is possible in DEM, a minimum separation $h_{\min}$ is assumed in the present paper. This is necessary in order to represent the physical repulsive nature between particles and avoid singular attractive force when h equals to zero [48].

B. Simulation conditions

A simulation began with the random generation of monosized spherical particles with no overlap in a rectangular box with width equals to ten particle diameter. Then, the particles were allowed to settle down under gravity and during this densification process, they would colloid with neighboring particles and bounce back and forth. The dynamic packing process proceeded until all particles reached their stable positions with an essentially zero velocity as a result of the damping effect for energy dissipation. Figure 2 shows snapshots at different times to illustrate the formation of a packing.

As reported elsewhere [46], the initial state before settling would not affect the final state of a packing. Nevertheless, to ensure consistent results, the porosity at the initial state was constant, set to 0.94 for all packings considered. Furthermore, periodical boundary conditions were applied along the two horizontal directions to avoid lateral wall effect. This treatment also allowed the formation of a more homogenous packing and helped generating enough data for analysis while using a small number of particles in a simulation.

TABLE I. Condition for the simulation of fine particle packing.

Parameter[a]	Value
Particle size, d	1–1000 μm
Particle density, ρ	2.5×10^3 kg m^{-3}
Number of particles, N	1024
Young's modulus, Y	1.0×10^7 N m^2
Poisson's ratio, $\tilde{\sigma}$	0.29
Friction coefficient, μ	0.3
Rolling friction coefficient, μ_r	0.002
Normal damping coefficient, γ_n	2×10^{-5}
Hamaker constant, H_a	6.5×10^{-20} J
Minimum separation, $h_{\min}$	1 nm

[a]It is assumed that the container has the same parameters as particles.

Table I lists the physical conditions and parameters for the present simulation, obtained after some trial tests. Since the present paper was focused on the effect of particle size, typical but constant material properties or parameters were used. The effect of the van der Waals force on particle packing can be observed when particle size is less than about 100 μm [19]. On the other hand, if particle size is less than 1 μm, other weak forces, e.g., electrostatic force, are also effective [15,48] but they were not included in the present calculation of the interparticle forces. Therefore, simulations were mainly performed for particles ranging from 1 to 100 μm. However, a few simulations were also performed for coarse particles up to 1000 μm in order to investigate the transition of packing structure from coarse to fine particles. The magnitude of time steps in the simulations varies with particle size [44], ranging from 1×10^{-10} to 7×10^{-7} s for the size range considered.

III. RESULTS AND DISCUSSION

Figure 3 shows the contact network of particles in the packing of particles of different sizes, which were, respectively, obtained by taking internal spherical samples whose sizes vary with particle size to be representative. It is obvious that the structure becomes looser and looser as particle size decreases, which is in agreement with the previous observation [17,18]. However, as pointed out earlier, proper quantification of the packing structures is necessary in order to enhance the present understanding. In the following, as a first step in this direction, the packing of fine particles will be analyzed in terms of most commonly used concepts such as porosity, radial distribution function, angular distribution, and coordination number. An attempt will also be made to relate packing properties to interparticle forces.

A. Porosity

Table II lists the porosity results for the packings simulated, which shows that porosity decreases as particle size increases. However, significant variation of porosity can only

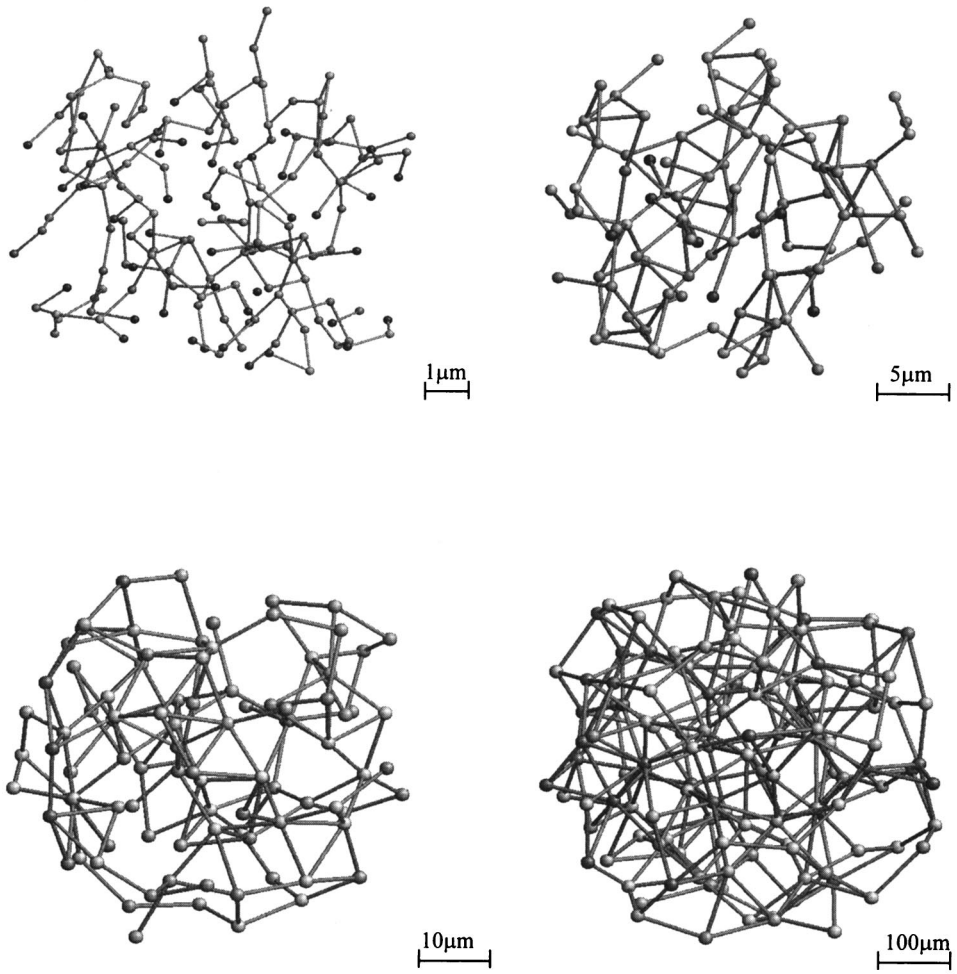

FIG. 3. The contact network in a spherical sample taken from the packing of different sized particles. Small balls represent the centers of particles, and sticks represent the contacts between particles.

be observed when particle diameter is less than about 100 μm. Porosity can be as high as 0.835 for particles of 1 μm, compared to 0.378 for 1000 μm particles. For coarse particles, porosity is known to have two limits: 0.36 for the random dense packing and 0.40 for the random loose packing [59,60]. The present simulation represents the so-called poured packing, with porosity of coarse particles equal to 0.378, well within the two limits as expected.

As shown in Fig. 4, the simulated results are quite comparable to the measurements of Milewski [17] and Feng and Yu [61]. This is also the case for other literature data summarized by Yu, Bridgwater, and Burbidge [19]. It should be pointed out that the packing of fine particles is affected by many variables related to material properties and particle characteristics, even for a given packing method. Early studies have not taken into account all these parameters, giving scattered results. On the other hand, it was noticed that the present simulation conditions are reasonably comparable to those used by Feng and Yu [61] who used glass beads in their experiment. Therefore, the good agreement between the simulated and measured results in Fig. 4 confirms that the physical conditions and parameters selected are indeed typical and macroscopically verifies the present approach. For the packing of coarse particles, as mentioned earlier, the validity of such a DEM-based simulation has been confirmed at both macroscopical and microscopic levels [45–47].

B. Radial distribution function

Radial distribution function $g(r)$ is the probability of finding the center of a particle at a given distance r from a reference one and is widely used in the study of particle packing as it contains useful information about the interparticle radial correlations [22,23]. For the purpose of comparison, normalized radial distribution functions was used in this paper. That is, $g(r)$ is given by

$$g(r)=\frac{dN(r)}{4\pi r^2 dr\rho_0}, \tag{9}$$

TABLE II. Mean packing properties for particles of different sizes.

Particle size (μm)	1	2	5	10	20	50	100	200	1000
Porosity $\varepsilon(-)$	0.835	0.783	0.674	0.580	0.539	0.457	0.409	0.387	0.378
Mean coordination number $\overline{N}(-)$	2.13	2.26	3.13	4.18	4.17	5.25	5.57	5.78	5.98

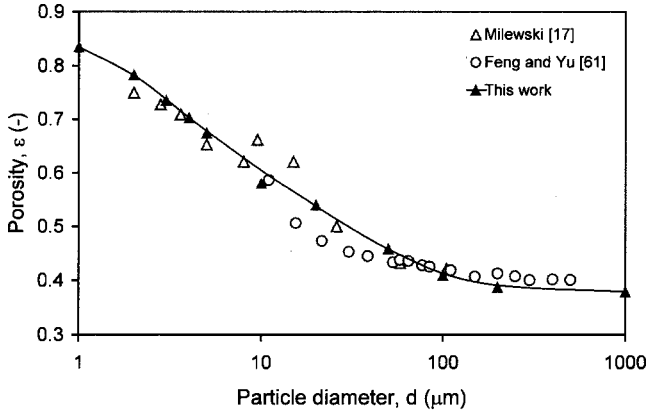

FIG. 4. Dependence of porosity on particle size: comparison between present simulation and experimental measurement [Refs. [17,61].

where $N(r)$ is the average number of particle centers within a spherical space with radii r around the center of a reference particle and ρ_0 is the average number of particle per unit volume in the packing, equal to $6(1-\varepsilon)/\pi$. Figure 5 shows $g(r)$ for different sized particles when $dr=0.02$. The $g(r)$ curve for particles of 1000 μm exhibits all the well-known short-range features observed in the random packing of hard particles [22,60]. In particular, it has the split second peak at the distance of 1.73 and 2.0, respectively, corresponding to two types of particle connection: (a) edge-sharing in-plane equilateral triangles and (b) three particles along a line, which is recognized as a key characteristic of a random packing of hard particles [60]. When particle size decreases, the following key changes can be identified. First, the first component of the second peak at $r=1.74$ vanishes when particle size is less than 100 μm although the main component at $r=2.0$ is maintained. Second, the peaks beyond the second one gradually vanish. Third, the first peak becomes narrower, with a sharp decrease to the first minimum. These changes suggest that decreasing particle size can result in a more uniform packing. In fact, for particles less than about 10 μm, the variation of radial distribution function is largely limited to a small distance ($r<2$). Notably, these changes differ from those reported by Yen and Chaki [21]. This difference is believed to result from the different simulation algorithms and conditions. For example, the rotational motion of particles was completely ignored in the work of Yen and Chaki. On the contrary, as will be reported elsewhere, the simulation based on the present algorithm indicated that not only the rotation but also the rolling friction significantly affect the simulated results.

The local structure has been further analyzed in terms of angular distribution function $P(\theta)$, which is focused on the connection angle between three contacting particles. For coarse particles, as shown in Fig. 6, $P(\theta)$ has two peaks: one strong peak at 60° and the other at 120°. As particle size decreases to about 50 μm, the peak at 120° disappears first. Then further decreasing particle size will gradually lead to the vanishing of the peak at 60°. The two peaks were considered to be linked to the so-called ''211'' and ''333'' configurations which, according to Clarke and Jonsson [40], provide dominant contributions to the second peak in the $g(r)$ curve. The vanishing of the two peaks in $P(\theta)$ implies decreased proportion of the two configurations in a packing; corresponding to this is the disappearing of the first component of the second peak and the shift of the first minimum in $g(r)$. Probably further analysis is required to verify this consideration.

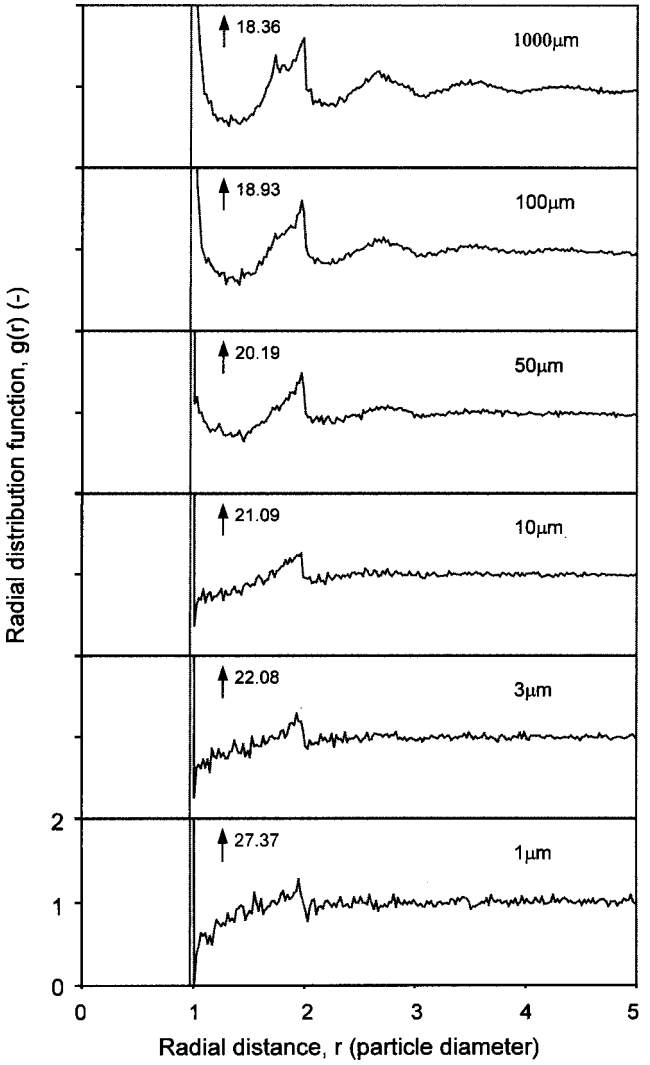

FIG. 5. Radial distribution function for packings of different sized particles.

C. Coordination number

Coordination number i.e., the number of ''contacts'' made by the particles, is considered to be a more sensitive measure of the local structure [3,60]. It varies significantly with the critical distance of separation less than which two particles are defined in contact. This is obvious from Fig. 7 that shows the number of particles N within a radial distance r of a reference particle, an alternative plot of radial distribution function but focused on small r. The angular distribution is also related to the contact condition between particles. In general, a small angle of contact corresponds to a high-coordination number.

Figure 8 shows the frequency distribution of coordination number when the critical distance of separation is set to 1.005 diameter. For coarse particles, coordination number varies from 3 to 10 and its frequency distribution is approxi-

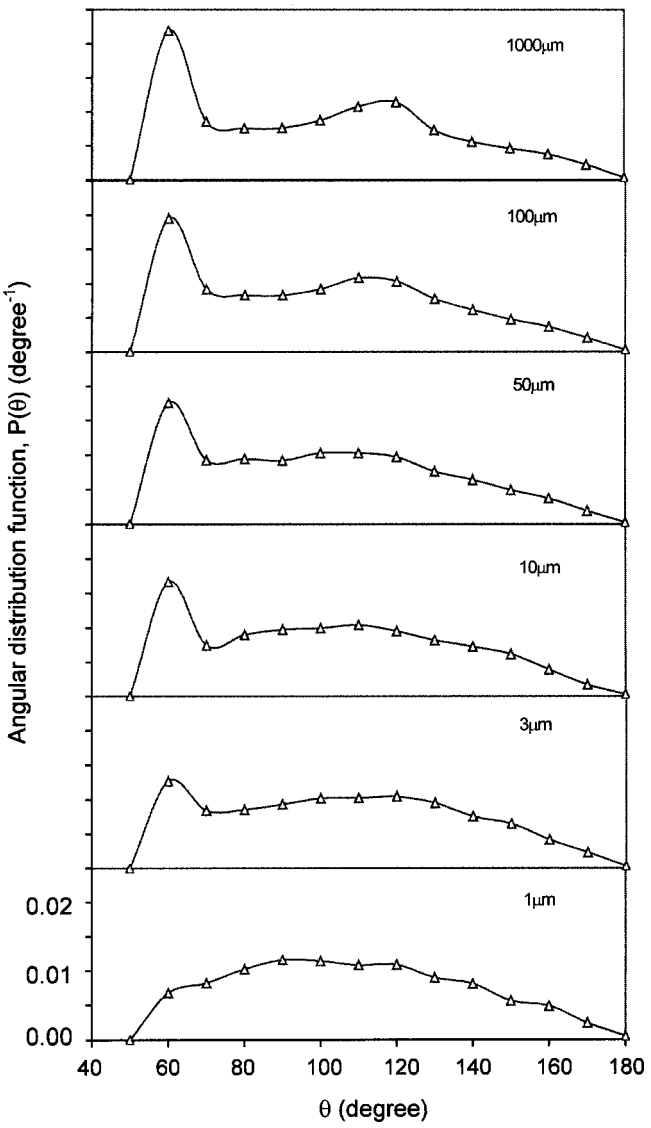

FIG. 6. Angular distribution $P(\theta)$ for packings of different sized particles.

mately symmetrical with its most probable value at 6, which is obviously comparable to those reported [22,60]. As particle size decreases, the distribution shifts towards to the left and becomes narrower and narrower. Notably, for 1 μm particles, the coordination number mostly varies from 1 to 4, with its most probable value equal to 2. The contact conditions for particles of different sizes can also be visualized in Fig. 3.

The mean coordination number varies with particle size, as also listed in Table II. For the packing of coarse particles where the gravity is dominant, a particle should have three supporting particles underneath and in turn support other three particles, giving a mean coordination number of value 6 [28,60]. However, for the packing of fine particles, this mechanical stability is not strict because the gravity force is not dominant. Instead, the van der Waals and friction forces are strong enough to counteract the gravity force; consequently the densification due to sliding and rolling between particles is significantly reduced. In that case, it is understandable that the coordination number can be decreased substantially. However, to maintain the continuity in both

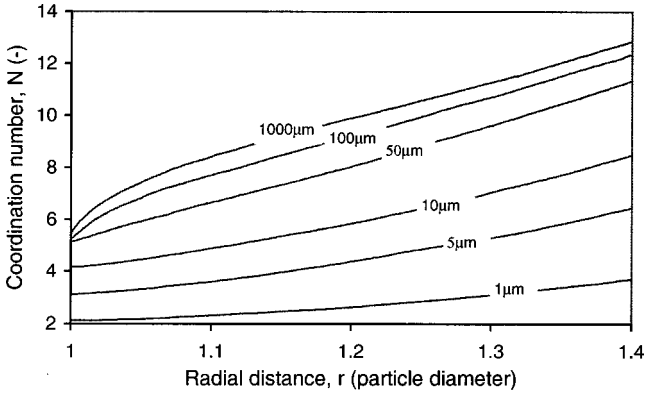

FIG. 7. The number of particle centers as a function of radial distance for different sized particles.

structure and force, a minimum contact is required. Thus, it is plausible that the minimum mean coordination number is equal to 2, in order that a particle can be supported by one particle and at the same time to support another. Corresponding to this is a chainlike packing structure shown in Fig. 3 for 1 μm particles.

It is generally accepted that for the packing of monosized particles, there is a correlation between mean coordination number and porosity [2]. Strictly speaking, such analysis is not so meaningful because different physical and/or packing conditions may have to be employed to vary porosity or coordination number [62]. This deficiency can be readily overcome by computer simulation. In particular, the present paper generates various packing under exactly the same conditions except for particle size. Figure 9 shows the results, indicating that the mean coordination number decreases with porosity. Interestingly, as a result of the loosening packing structure, the change of the critical distance of separation mainly affects the results for small porosity. It was also found that the relationship between the mean coordination number $\overline{N}$ and porosity ε can be satisfactorily described by the following equation:

$$\overline{N}=\overline{N}_0\frac{1+m(1-\varepsilon)^4}{1+n(1-\varepsilon)^4}. \tag{10}$$

Parameters $\overline{N}_0$, m, and n are, respectively, 2.02, 87.38, and 25.81 when the critical distance of separation is 1.005. Note

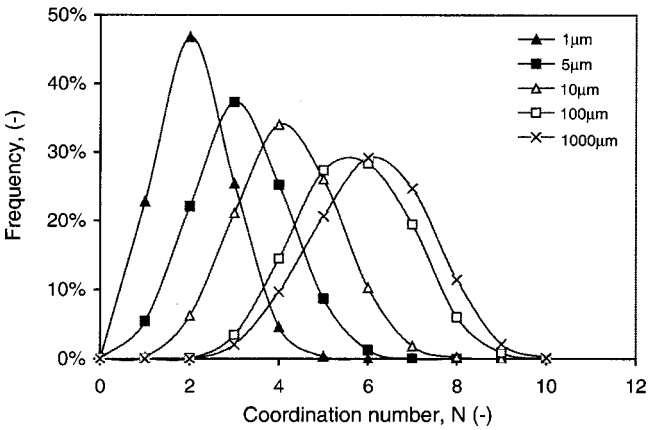

FIG. 8. Coordination number distribution for different sized particles.

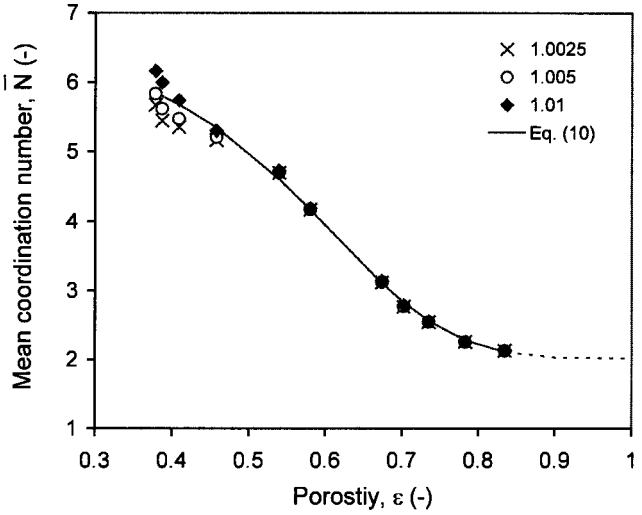

FIG. 9. Variation of mean coordination number with porosity for different critical distance of separation.

that while the $\overline{N}-\varepsilon$ relation is consistent with those reported elsewhere [2,62], the present paper covers a wider porosity range. Porosity as high as 0.997 is possible for nanoparticles [18]. However, from the arguments mentioned above, the most probable coordination number is two for ultrafine particles and the limiting mean coordination number $\overline{N}_0$ when $\varepsilon=1.0$ should be close to this value, equal to 2.02 as suggested by Eq. (10).

D. Force distribution

One important feature of a dynamic simulation is that interparticle force information can be readily quantified. In this case, it is possible to examine the relationship between interparticle force and packing structure. As implied by Eq. (3), three forces are effective here: contact force $\mathbf{F}_{ij}^c(=\mathbf{F}_{ij}^n+\mathbf{F}_{ij}^s)$, van der Waals force $\mathbf{F}_{ij}^v$, and gravity $m\mathbf{g}$. Different from the gravity, $\mathbf{F}_{ij}^c$ and $\mathbf{F}_{ij}^v$ have no preferential direction; instead, they should be randomly oriented in a packing. As such, there may be different ways to evaluate their representative magnitudes or values acting on individual particles for the purpose of comparison. Two force ratios were used in this paper because of their obvious physical meaning. For the van der Waals force, they are, respectively, defined by

$$\chi_v=\left|\sum_j \mathbf{F}_{ij}^v\right| \Big/ m_i g \tag{11}$$

and

$$\chi_v'=\sum_j |\mathbf{F}_{ij}^v| \Big/ m_i g. \tag{12}$$

The two definitions are also applied to the contact force $\mathbf{F}_{ij}^c$, accordingly giving χ_c and χ_c'. Figures 10 and 11 show the probability density distributions for the contact and ver der Waals forces for different sized particles. They are in terms of definition (11) but with logarithmic scale. Similar distributions were also found in terms of definition (12).

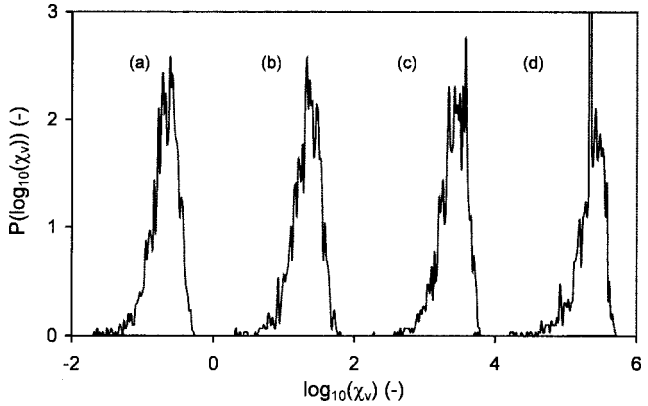

FIG. 10. The probability density distribution $P(\log_{10}\chi_v)$ of the van der Waals force relative to the gravity for different sized particles: (a) 1000 μm; (b) 100 μm; (c) 10 μm, and (d) 1 μm.

As expected, the van der Waals force relative to the gravity force in a packing increases with the decrease of particle size. The ratio of the contact force to the gravity force will accordingly increase in order to create a repulsive force to maintain the mechanical equilibrium. As suggested in Fig. 10, there may be a similarity in the distribution of the van der Waals forces. Such a similarity is also observed for the contact force for fine particles less than 100 μm, as shown in Fig. 11. However, coarse particles give a contact force distribution quite different from that of fine particles. In fact, the probability density distribution of the contact forces for 1000 μm particles has a broader distribution, with the order of magnitude equal to 4 and comparable to that for dense two-dimensional packings [63]. However, the force range reduces to two orders of magnitude for fine particles. Another important feature here is that the contact force distribution is similar to the van der Waals force distribution for particles less than 100 μm. This similarity reflects the dominant role of the van der Waals force, as the contact force is the passive force and can only respond to the active force, i.e., van der Waals force in this case.

The packing state must be linked to the interparticle force in some way. With this realization, Feng and Yu [64] recently quantified the relationship between porosity and capillary force, which is dominant for the packing of wet coarse

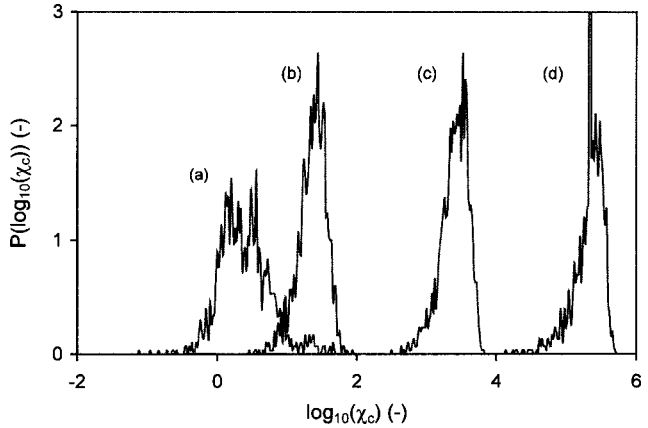

FIG. 11. The probability density distribution $P(\log_{10}\chi_c)$ of the contact force relative to the gravity for different sized particles: (a) 1000 μm, (b) 100 μm, (c) 10 μm, and (d) 1 μm.

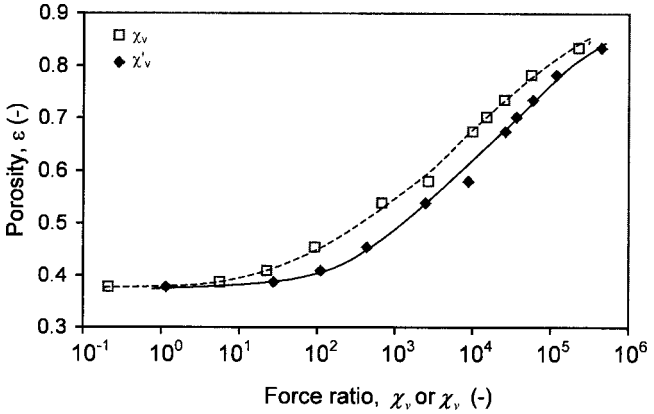

FIG. 12. Porosity as a function of the force ratio defined by Eqs. (11) or (12).

particles. Based on the present results, such a relationship can also be established for the packing of fine particles when the van der Waals force is dominant. As shown in Fig. 12, this relationship can be given by

$$\varepsilon = \varepsilon_0 + (1-\varepsilon_0)\exp(\alpha \chi^{\beta}), \tag{13}$$

where ε_0 is the initial porosity of random packing of hard particles, corresponding to the porosity when the van der Waals force is completely negligible. Two sets of parameters α and β were obtained, i.e., -7.750 and -0.256 corresponding to Eq. (11), -14.278 and 0.2916 corresponding to Eq. (12), although $\varepsilon_0 = 0.386$ for both cases. It is obvious from Fig. 12 that porosity increases with the force ratio; however, this increase becomes significant only when the van der Waals force is much larger than the gravity force. This is probably due to the fact that unlike the gravity, there is no preferred direction in the van der Waals force because of the random arrangement of particles. As such, it becomes effective only when it is large enough to provide a resistance force to restrict the relative movement between particles in forming a packing under given conditions.

IV. CONCLUSIONS

It has long been proposed that long-range interparticle forces, e.g., the van der Waals and electrostatic forces, play an essential role in the packing of fine particles. However, because of the difficulty in measuring these forces and/or packing structure, it is still unable to quantify experimentally the packing structure in relation to particle size and these forces. In this paper, we have shown this difficulty can be overcome by the use of DEM-based dynamic simulation. The effect of particle size ranging from 1 to 1000 μm on particle packing has been quantified in terms of the most commonly used concepts such as porosity, radial distribution function, angular distribution, and coordination number. The three-dimensional chainlike structure of fine particles is depicted and quantified. The relationship between porosity and van der Waals force has also been established, which is believed to be useful in linking macroscopic to microscopic properties for the packing of fine particles.

ACKNOWLEDGMENT

The authors are grateful to the Australian Research Council for financial support of this work.

[1] W. A. Gray, *The Packing of Solid Particles* (Chapman and Hall, London, 1969).
[2] R. M. German, *Particle Packing Characteristics* (Metal Powder Industries Federation, Princeton, NJ, 1989).
[3] J. D. Bernal, Proc. R. Soc. London, Ser. A **284**, 299 (1964).
[4] A. Angell, J. H. R. Clarke, and L. V. Woodcock, Adv. Chem. Phys. **48**, 397 (1981).
[5] W. B. Fuller and S. E. Thompson, Trans. Am. Soc. Civ. Eng. **59**, 67 (1907).
[6] A. B. Yu and R. P. Zou, KONA Powder Particle **16**, 68 (1998).
[7] J. A. Dodds, J. Colloid Interface Sci. **77**, 317 (1980).
[8] N. Ouchiyama and T. Tanaka, Ind. Eng. Chem. Fundam. **25**, 125 (1986).
[9] T. Stovall, F. De Larrard, and M. Buil, Powder Technol. **48**, 1 (1986).
[10] A. B. Yu and N. Standish, Powder Technol. **55**, 71 (1988).
[11] A. B. Yu and N. Standish, Ind. Eng. Chem. Res. **30**, 1372 (1991).
[12] A. B. Yu, R. P. Zou, and N. Standish, J. Am. Ceram. Soc. **75**, 2765 (1992).
[13] R. P. Zou and A. B. Yu, Powder Technol. **88**, 71 (1996).
[14] A. B. Yu, R. P. Zou, and N. Standish, Ind. Eng. Chem. Res. **35**, 3730 (1996).
[15] J. Visser, Powder Technol. **58**, 1 (1989).
[16] R. Roller, Ind. Eng. Chem. **22**, 1207 (1930).
[17] J. V. Milewski, *Handbook of Fillers and Reinforcements for Plastics*, edited by J. V. Milewski and H. S. Katz (Van Nostrand Reinhold, New York, 1987), pp. 14–33.
[18] M. Mizuno, A. Fukaya, and G. Jimbo, KONA Powder Particle **9**, 19 (1991).
[19] A. B. Yu, J. Bridgwater, and A. Burbidge, Powder Technol. **92**, 185 (1997).
[20] C. L. Feng, R. P. Zou, and A. B. Yu, Proceedings of the 6th International Conference *On Bulk Materials Storage, Handling and Transportation, 1998* (Institution of Engineers, Australia, Barton ACT, 1998), pp. 389–396.
[21] K. Z. Y. Yen and T. K. Chaki, J. Appl. Phys. **71**, 3164 (1992).
[22] *Disorder and Granular Media*, edited by D. Bideau and A. Hansen (North-Holland, Amsterdam, 1993).
[23] *Granular Matter: An Interdisciplinary Approach*, edited by A. Mehta (Springer, New York, 1993).
[24] E. M. Tory, N. A. Cochrane, and S. R. Waddell, Nature (London) **220**, 1023 (1968).
[25] W. M. Visscher and M. Bolsterli, Nature (London) **239**, 504 (1972).
[26] E. M. Tory, B. H. Church, M. K. Tam, and M. Ratner, Can. J. Chem. Eng. **51**, 484 (1973).
[27] C. H. Bennett, J. Appl. Phys. **432**, 727 (1972).
[28] D. J. Adams and A. J. Matheson, J. Chem. Phys. **56**, 1989 (1972).

[29] A. J. Matheson, J. Phys. C **7**, 2569 (1974).
[30] D. S. Boudreaux and J. M. Gregor, J. Appl. Phys. **48**, 158 (1977).
[31] M. J. Powell, Powder Technol. **25**, 45 (1980).
[32] P. Meakin and R. Jullien, J. Phys. (France) **46**, 1543 (1985).
[33] K. E. Thompson and H. S. Fogler, AIChE J. **43**, 1377 (1997).
[34] N. D. Aparicio and A. C. F. Cocks, Acta Metall. Mater. **43**, 3873 (1995).
[35] J. L. Finney, Mater. Sci. Eng. **23**, 199 (1976).
[36] W. S. Jodrey and E. M. Tory, Phys. Rev. A **32**, 2347 (1985).
[37] A. S. Clarke and J. D. Wiley, Phys. Rev. B **35**, 7350 (1987).
[38] G. T. Nolan and P. E. Kavanagh, Powder Technol. **72**, 149 (1992).
[39] G. C. Barker and A. Mehta, Phys. Rev. A **45**, 3435 (1992).
[40] A. S. Clarke and H. Jonsson, Phys. Rev. E **47**, 3975 (1993).
[41] R. Jullien, P. Jund, D. Caprion, and D. Quitmann, Phys. Rev. E **54**, 6035 (1996).
[42] A. Yang, C. T. Miller, and L. D. Turcoliver, Phys. Rev. E **53**, 1516 (1996).
[43] D. He, N. N. Ekere, and L. Cai, Phys. Rev. E **60**, 7098 (1999).
[44] P. A. Cundall and O. D. L. Stack, Geotechnique **29**, 47 (1979).
[45] Z. P. Zhang, R. P. Zou, A. B. Yu, P. Langston, and K. D. Kafui, *Proceedings Chemeca 97, Rotorua, NZ, 1997* (Institution of Professional Engineers, New Zealand, 1997), pp. 263–270 (Particle Technology).
[46] L. F. Liu, Z. P. Zhang, and A. B. Yu, Physica A **268**, 433 (1999).
[47] Z. P. Zhang, L. F. Liu, and A. B. Yu, Powder Technol. (to be published).
[48] J. N. Israelachvili, *Intermolecular and Surface Forces*, 2nd ed. (Academic, London, 1991).
[49] M. P. Allen and D. J. Tildesley, *Computer Simulation of Liquids* (Clarendon, 1987).
[50] K. L. Johnson, *Contact Mechanics* (Cambridge University Press, Cambridge, 1985).
[51] N. V. Brilliantov, F. Spahn, J. M. Hertzsch, and T. Pöschel, Phys. Rev. E **53**, 5382 (1996).
[52] T. Schwager and T. Pöschel, Phys. Rev. E **57**, 650 (1998).
[53] R. D. Mindlin and H. Deresiewicz, J. Appl. Mech. **20**, 327 (1953).
[54] P. A. Langston, U. Tüzün, and D. M. Heyes, Chem. Eng. Sci. **50**, 967 (1995).
[55] F. P. Beer and E. R. Johnson, *Mechanics for Engineers-Statics and Dynamics* (MacGraw-Hill, New York, 1976).
[56] N. V. Brilliantov and T. Pöschel, Europhys. Lett. **42**, 511 (1998).
[57] Y. C. Zhou, B. D. Wright, R. Y. Yang, B. H. Xu, and A. B. Yu, Physica A **269**, 536 (1999).
[58] H. C. Hamaker, Physica (Amsterdam) **4**, 1058 (1937).
[59] G. D. Scott, Nature (London) **194**, 956 (1962).
[60] J. L. Finney, Proc. R. Soc. London, Ser. A **319**, 479 (1970).
[61] C. L. Feng and A. B. Yu, Powder Technol. **99**, 22 (1998).
[62] D. Pinson, R. P. Zou, A. B. Yu, P. Zulli, and M. McCarthy, J. Phys. D **31**, 457 (1998).
[63] F. Radjai, M. Jean, J. J. Moreau, and S. Roux, Phys. Rev. Lett. **77**, 274 (1996).
[64] C. L. Feng and A. B. Yu, J. Colloid Interface Sci. (to be published).